

## ASSESSMENT OF SHALLOW WATER PERFORMANCE USING INTERFEROMETRIC SONAR COHERENCE

Stig A. Synnes, Roy E. Hansen, Torstein O. Sæbø

Norwegian Defence Research Establishment (FFI), PO Box 25, N 2027 Kjeller, Norway

Contact author: Stig A. Synnes, e-mail: Stig-Asle.Synnes@ffi.no, fax: +47 63807509

**Abstract:** *Interferometry is used for bathymetric mapping with side scan and synthetic aperture sonars. The principle is based on estimating the time difference between arrivals for two vertically displaced receivers. An important additional feature with interferometric sonar is that an estimate of the signal-to-noise ratio can be derived from the coherence between overlaid data series from the two receivers. Interferometric sonar coherence therefore allows for an effective real-time estimate of quality for side scan sonar and synthetic aperture sonar measurements.*

*We have conducted a series of trials in shallow waters along with Kongsberg Maritime using a HISAS 1030 interferometric sonar mounted on a HUGIN autonomous underwater vehicle. We have also developed a tool for shallow water performance assessment based on a simple ray model. In this paper we first demonstrate how the interferometric sonar coherence relates to the image quality of synthetic aperture images. We then associate the coherence from real data with results from the model in order to better understand the different signal contributions. For the shallow water environment of investigation, we identify multipath returns as the limiting factor for image quality.*

*We conclude that the interferometric sonar coherence yields an effective estimate of quality for interferometric side scan sonar and synthetic aperture sonar measurements. It allows for a simple real-time estimate of the imaging range and in combination with simulations provides the means required for autonomous on-the-fly change of the sonar geometries and settings for optimal performance.*

**Keywords:** *Sonar performance, cross-correlation, coherence, very shallow waters*

## 1. BACKGROUND

Side scan sonar (SSS) and synthetic aperture sonar (SAS) are two important technologies for imaging the seafloor. In very shallow waters their performance strongly depends on the environmental conditions. A primary source for this limitation is the contamination of the returned signal by multipath returns. The identification of dominating multipaths has earlier been investigated through advanced experiments [1][2]. In this paper we combine measurements with a dedicated model description in order to relate the loss of performance to the correct source and environmental condition.

## 2. MEASUREMENTS

We have conducted a series of measurements in very shallow waters along with Kongsberg Maritime using a HISAS 1030 interferometric sonar [3] mounted on a HUGIN autonomous underwater vehicle. In Fig. 1 we present two sample images from the same scene with water depth around 9 m. While the first image has good quality all the way out to 150 m range, the quality of the second image is poor above roughly 55 m range. In Fig. 2 we present a measurement-based signal-to-noise ratio (SNR) of the data used to generate the two images and observe that the image degradation corresponds to a decrease of the SNR that at 55 m range crosses roughly 2 dB.

For AUV operations the capability of estimating the imaging range and if possible optimise the sonar performance can be of great importance. We will adopt the SNR of the beamformed signal as a measure of imaging potential and identify the main limiting factors to the SNR.

The measurement-based SNR is obtained from the time series of the two vertically displaced arrays of the interferometric sonar. Assuming a Gaussian distribution of both signal and noise amplitudes, the SNR is given by the maximum normalised correlation factor  $\mu$ , the coherence, when correlating the two time series [4]:

$$SNR = \frac{\mu}{1 - \mu}$$

## 3. MODEL

We have developed a ray tracing tool for modelling the SNR in shallow waters. The SNR is estimated from the ratio of the direct bottom return to the sum of all other returns, including the direct surface return and returns involving two or more reflections from bottom and surface. A simplification is adopted in that only one non-specular reflection is allowed for each ray. This significantly reduces the computational task, while preserving a reasonable accuracy as most of the energy is reflected around the specular direction. The performance of the model is indicated by the similarity between the measured and modelled SNR of Fig. 2.

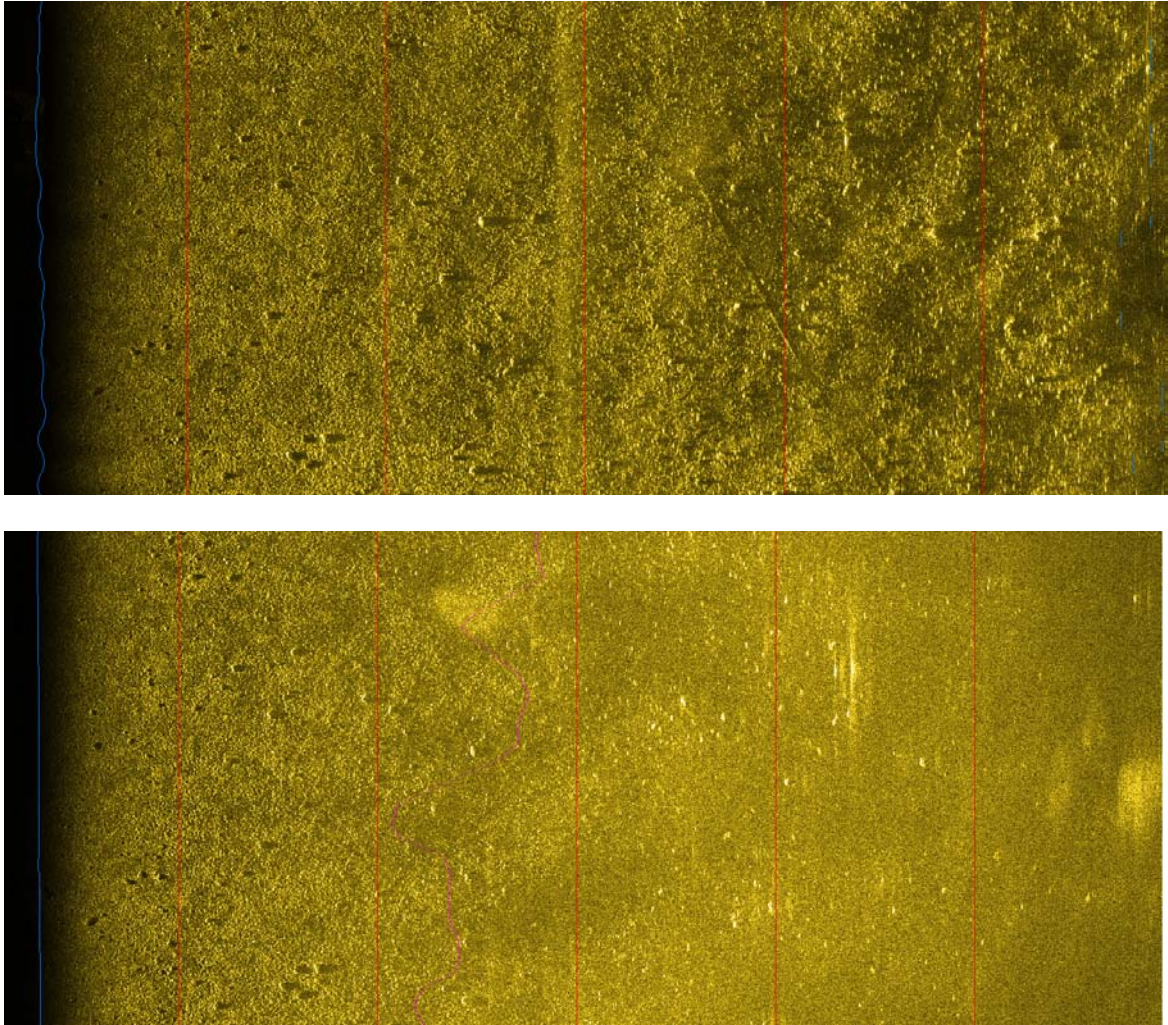


Fig.1: Two SAS images taken one week apart of the same scene by HISAS 1030 on a HUGIN AUV using identical settings. The water depth is 9 m and the vehicle depth 3 m. The range spans from 0 m to 150 m from left to right. The main environmental change is a reduction of the wind speed from 13 m/s of the upper image to 4 m/s of the lower image.

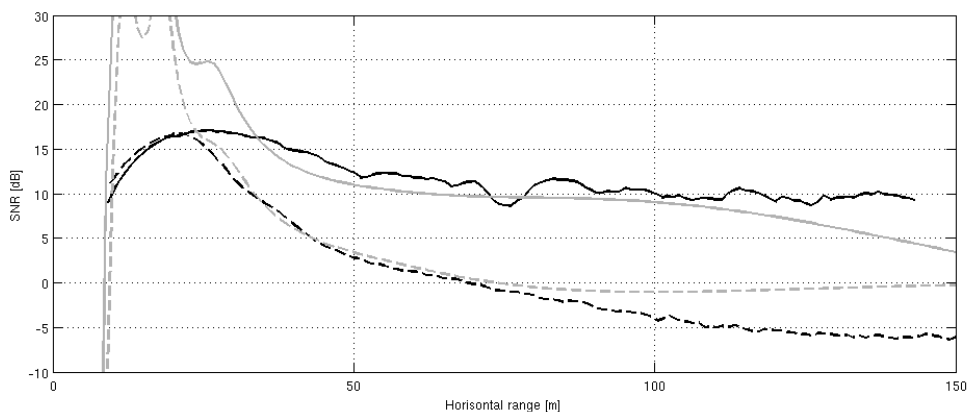


Fig.2: The measurement-based SNR for beamformed (sidescan) lines of sonar data (i.e. prior to SAS image processing) is presented in black. The solid and dashed lines give the results for the good and poor image respectively. The grey lines correspond to simulations for the environmental conditions of the two measurement campaigns.

The raytracer is based upon the analytic solution for piecewise constant gradient of the sound speed from [6], sec 6.2. For bistatic bottom scattering we selected Ellis' model [7] combining Lambert scattering valid for intermediate angles with a facet term for specular reflection. The model is extended to smaller grazing angles by including Del Balzos platou as a correction term to the Lambert scattering [8]. For bistatic surface scattering we choose the APL-UW94 backscattering model [9] as a basis and performed a brute expansion to a bistatic model by mimicking the layout of Ellis' model. The model results show good resemblance in forward and back-scattering benchmarking. Finally additive noise is mimicked by adding a noise level that prevents the sensor from obtaining a SNR of more than 0 dB at 300 m.

In the model computations we assume bottom consisting of gravel (as indicated from the SAS-image), adopt wave height estimated from wind strength, and a sound speed profile recorded with a CTD profiler. The sonar is simulated with a transmitter beamwidth of  $15^\circ$  steered  $15^\circ$  below the horizontal plane and a receiver beamwidth of  $28^\circ$  centred around  $22^\circ$  below the horizontal plane.

#### 4. ANALYSIS

The modelled SNR were presented together with the measurement-based SNR in Fig. 2, and a good resemblance between the two can be observed, in particular in the range interval of 30 m to 100 m. We believe that the discrepancies at longer range are effects of the increasing sensitivity to inaccurate assessments of the sound speed profile, additive noise, bathymetry and/or bottom type for long range and very small grazing angles. The discrepancies between measurements and model at short range we believe is related to a combination of an overestimated modelled SNR and an underestimated measurement-based SNR. The modelled SNR is unrealistic high in some areas where the direction of the multipaths coincide with zeros in the transmitter or receiver beampatterns. The resulting complete loss of a multipath only occurs in our simplified 2D model, as both a 3D model and inclusion of diffuse scattering at all interfaces would smooth the directivity of the contributions. Furthermore, the SNR estimated from coherence measurements is possibly too low in the short range region. This could be caused by baseline decorrelation and processing induced decorrelation [5], and will be investigated further.

We now return to the two images and try to identify the effect causing the huge difference in their SNRs. By adjusting one parameter of the modelled environments at a time and evaluating the related effect on the SNR, we observe that the main origin of the changing SNR is the different sea states of the two days with wind speeds of 13 m/s for the good image and 4 m/s for the poor image.

Multiple paths with the same round-trip distance are characterised by their different angles out of the transmitter and into the receiver, as illustrated by the round-trip paths in the bottom panel of Fig. 3. By shaping the transmitter and receiver beam patterns beneficially, it is therefore possible to reduce the effect of undesired multipaths. In Fig. 3 we visualize the contribution of the dominating multipaths for the modelled sonar and environments. All multipaths contributing 10% or more to the total contribution at any distance is included in the figure, with the results for the good quality image in the top panel, and the poor quality image in the centre panel. The individual multipaths of each colour are illustrated for one roundtrip distance in the lower panel. We observe that the relative contribution of the multipaths are stronger in the poor quality image, and that multipaths with two bottom and one surface scattering give the main contributions to the SNR in our examples. Under windy

conditions a better imaging range is achieved, probably as a result of damping and spreading of the multipath returns at the surface.

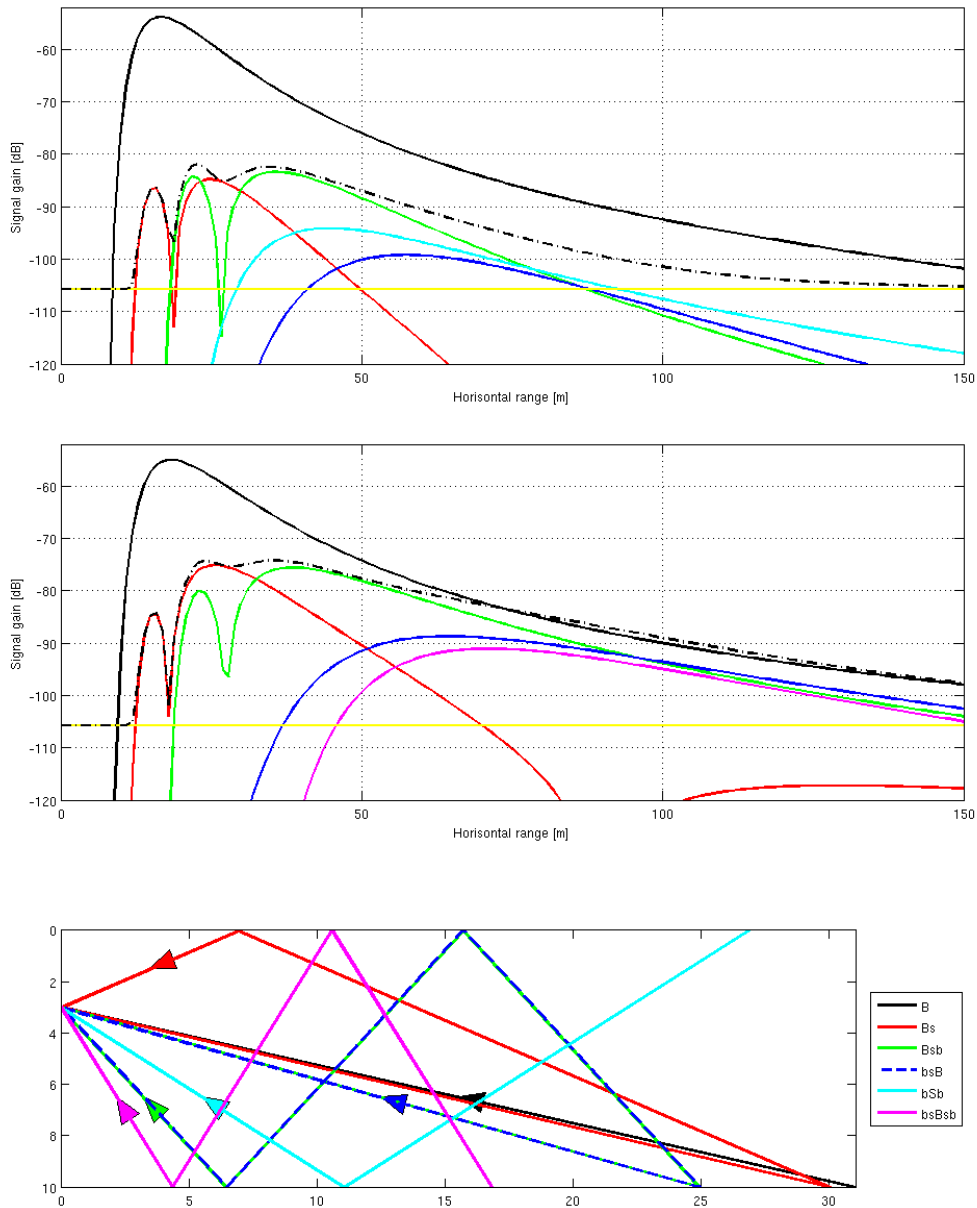


*Fig.3: Individual multipath contributions of the images for windy and calm conditions in the top and centre panels respectively. The direct return is indicated with the black solid line and the total multipath contribution with the black dotted line. Furthermore, all multipaths contributing 10% or more to the total multipath contribution are plotted in different colours. The yellow line indicates an assumed additive noise floor. The lower panel indicates the path corresponding to each colour, exemplified for round-trip ray paths of 65 m length. The paths are also indicated by the legend, stating the order of bottom (b/B) and surface (s/S) scatterings for each colour, and with the single non-specular scattering indicated by an uppercase letter.*

## 5. CONCLUSION

We conclude that the interferometric sonar coherence yields an effective estimate of quality for interferometric side scan sonar and synthetic aperture sonar measurements. It allows for a simple real-time estimate of the imaging range and in combination with simulations provides the means required for autonomous on-the-fly change of the sonar geometries and settings for optimal performance.

## REFERENCES

- [1] **A. Bellettini, M. Pinto, L. Wang**, Effect of multipath on synthetic aperture sonar, WUC 2003, Paris, 2003.
- [2] **L. S. Wang, G. Davies, A. Bellettini, M. A. Pinto**, A preliminary study of the effect of multipath on synthetic aperture sonar, Saclantcen memorandum, serial no: SM-401, 2003.
- [3] **P. E. Hagen, T. G. Fossum, R. E. Hansen**, The next generation mine hunting sonar for AUVs, In *Proceedings of UDT Pacific 2008*, Sidney, Australia, November 2008.
- [4] **H. A. Zebker, J. Villasenor**, Decorrelation in interferometric radar echoes, *IEEE Trans. Geosci. Remote Sensing.*, vol. 30, no. 5, pp. 950–959, 1992.
- [5] **R. Hanssen**, *Radar interferometry: Data interpretation and error analysis*, Kluwer Academic Press, 308 pages, 2001.
- [6] **L. J. Ziomek**, *Underwater acoustics – A linear systems theory approximation*, Academic Press, Orlando, Florida, 1985.
- [7] **D. D. Ellis, D. V. Crowe**, Bistatic reverberation calculations using three-dimensional scattering function, *J. Acoust. Soc. Am.*, pp. 2207-2214, 89 (5), 1991.
- [8] **D. R. Del Balzo, J. H. Leclerce, M. J. Collins**, Critical angle and seabed scattering issues for active-sonar performance predictions in shallow water, in *High frequency acoustics in shallow water*, Saclantcen conf. proc. series CP-45, 1997.
- [9] **APL-UW**, High-frequency ocean environmental acoustic models handbook, Applied Physics Laboratory, University of Washington, Seattle, Washington, technical report APL-UW TR 9407, 1994.